

PSR J0357+3205: a fast moving pulsar with a very unusual X-ray trail.

A. De Luca^{1,2}, R. P. Mignani^{1,3,4}, M. Marelli¹, D. Salvetti^{1,5}, N. Sartore¹, A. Belfiore⁶,
P. Saz Parkinson⁶, P.A. Caraveo^{1,2}, G.F. Bignami^{7,1}

deluca@iasf-milano.inaf.it

Received _____; accepted _____

¹INAF - Istituto di Astrofisica Spaziale e Fisica Cosmica Milano, Via E. Bassini 15, 20133 Milano, Italy

²Istituto Nazionale di Fisica Nucleare, Sezione di Pavia, Via Bassi 6, 27100 Pavia, Italy

³Mullard Space Science Laboratory, University College London, Holmbury St. Mary, Dorking, Surrey, RH5 6NT, UK

⁴Kepler Institute of Astronomy, University of Zielona Góra, Lubuska 2, 65-265, Zielona Góra, Poland

⁵Università degli Studi di Pavia, Dipartimento di Fisica, Via Bassi 6, 27100 Pavia, Italy

⁶Santa Cruz Institute for Particle Physics, Department of Physics, University of California at Santa Cruz, Santa Cruz, CA 95064, USA

⁷Istituto Universitario di Studi Superiori di Pavia, Piazza della Vittoria n.15, 27100 Pavia, Italy

ABSTRACT

The middle-aged PSR J0357+3205 is a nearby, radio-quiet, bright γ -ray pulsar discovered by the Fermi mission. Our previous *Chandra* observation revealed a huge, very peculiar structure of diffuse X-ray emission, originating at the pulsar position and extending for $> 9'$ on the plane of the sky. To better understand the nature of such a nebula, we have studied the proper motion of the parent pulsar. We performed relative astrometry on *Chandra* images of the field spanning a time baseline of 2.2 yr, unveiling a significant angular displacement of the pulsar counterpart, corresponding to a proper motion of $0''.165 \pm 0''.030 \text{ yr}^{-1}$. At a distance of $\sim 500 \text{ pc}$, the space velocity of the pulsar would be of $\sim 390 \text{ km s}^{-1}$ assuming no inclination with respect to the plane of the sky. The direction of the pulsar proper motion is perfectly aligned with the main axis of the X-ray nebula, pointing to a physical, yet elusive link between the nebula and the pulsar space velocity. No optical emission in the H_α line is seen in a deep image collected at the Gemini telescope, which implies that the interstellar medium into which the pulsar is moving is fully ionized.

Subject headings: Stars: neutron — pulsars: general — pulsars: individual (PSR J0357+3205)

1. Introduction

The Large Area Telescope onboard the *Fermi* satellite (*Fermi*-LAT, Atwood et al. 2009) has opened a new era for pulsar astronomy, by detecting γ -ray pulsations (at $E > 100$ MeV) from more than 120 pulsars¹, about 30% of which are not detected at radio wavelengths. The middle-aged PSR J0357+3205 (characteristic age $\tau_C \sim 0.54$ Myr) is one of the most interesting radio-quiet pulsars discovered in blind periodicity searches in *Fermi*-LAT data (Abdo et al. 2009a). Its high γ -ray flux (it is included in the *Fermi*-LAT bright source list, Abdo et al. 2009b), low spin-down luminosity ($\dot{E}_{rot} = 5 \times 10^{33}$ erg s⁻¹) and off-plane position (Galactic latitude $b \sim -16^\circ$) point to a small distance of about 500 pc. We investigated the field of PSR J0357+3205 with a joint X-ray and optical program with *Chandra* and the NOAO Mayall 4m telescope at Kitt Peak. This allowed us to identify the soft X-ray counterpart of the pulsar as an unremarkable source, looking fainter (and colder) than other well known middle-aged pulsars (De Luca et al. 2011). More interestingly, our deep *Chandra* observation unveiled the existence of a very large, elongated feature of diffuse X-ray emission, apparently originating at the pulsar position and extending for more than $9'$ (corresponding to ~ 1.3 pc at the distance of 500 pc, assuming no inclination with respect to the plane of the sky), with a hard spectrum consistent both with a power law and with a hot thermal bremsstrahlung.

Elongated “tails” of diffuse emission have been associated with several rotation-powered pulsars (e.g. Kargaltsev & Pavlov 2008) and explained as bow-shock pulsar wind nebulae (see Gaensler & Slane 2004, for a review), where their elongated morphology is “velocity-driven”. Indeed, if the pulsar moves supersonically through the interstellar medium, the termination shock of the pulsar wind assumes a “bullet” morphology, due to ram pressure. Particles accelerated at the shock emit synchrotron radiation and cool down,

¹See <https://confluence.slac.stanford.edu/display/GLAMCOG/Public+List+of+LAT-Detected+>

confined by ram pressure in an elongated region aligned with the pulsar space velocity. However, explaining the nature of the nebula associated with PSR J0357+3205 turned out to be very challenging. As discussed by De Luca et al. (2011), the standard picture cannot apply here since the morphology is very different from the “cometary” shape which characterizes all other X-ray bow-shock nebulae. There is no emission in the surroundings of the pulsar, where the brightest portion (the termination shock) should be – indeed, the surface brightness grows as a function of the distance from PSR J0357+3205. Moreover, there are no evidences for spectral evolution as a function of the position, at odds with expectations for a population of particles injected at the shock and cooling via synchrotron radiation.

Other pictures could be explored. For instance, PSR B2224+65, the fast moving pulsar powering the well known “Guitar nebula” seen in H_α (Cordes et al. 1993), displays an elongated X-ray feature which is reminiscent of the one of our target and cannot be a bow-shock nebula because it is misaligned by $\sim 118^\circ$ with respect to the direction of the proper motion (Hui & Becker 2007). Thus, the possibility of a ballistic jet (similar to Active Galactic Nuclei), or the hypothesis of a nebula confined by a pre-existing, large scale magnetic field in the interstellar medium have been proposed (Bandiera 2008; Johnson & Wang 2010; Hui et al. 2012).

Indeed, a crucial piece of information in order to understand the physics of the huge elongated feature associated with PSR J0357+3205 is the direction of the pulsar proper motion. Detecting a pulsar angular displacement aligned with the nebula’s main axis would link the morphology of the diffuse structure to the pulsar velocity. Conversely, if it were misaligned, the case of PSR J0357+3205 would become very similar to the one of PSR B2224+65 and would require a different explanation for the nature of the nebula.

Usually, a pulsar proper motion is measured in the radio band, or, more rarely, in the

optical domain. Unfortunately, our target is radio-quiet and has no optical counterpart; moreover, timing analysis of gamma-ray photons is not particularly sensitive to the proper motion (positional accuracy based on 5 yr of *Fermi*-LAT timing is estimated to be $\sim 2''$, Ray et al. 2011). The only way to search for a possible proper motion rests on the comparison of multi-epoch, high-resolution X-ray images. To this aim, we have obtained a multi-cycle observing campaign with *Chandra*, consisting of two observations to be performed at the end of 2011 and at the end of 2013. We will report here on the first observation of our program, as well as on a very recent observation of the field in the H_α band performed with GMOS instrument at the Gemini North telescope. Indeed, pulsars moving supersonically into warm interstellar gas can generate optical emission in the H_α line, due to collisional excitation of neutral hydrogen and charge exchange occurring at (and behind) the forward shock (see e.g. Cordes et al. 1993), yielding a limb-brightened, arc-shaped bow-shock nebula, located at the apex of the forward shock, in the direction of the proper motion.

2. Measurement of the pulsar proper motion

The superb angular resolution of the *Chandra* optics makes it possible to measure tiny angular displacements of an X-ray source by performing relative astrometry on multi-epoch images. Indeed, such an approach has already been used to measure the proper motion of a few isolated neutron stars. See e.g. our investigation for the case of SGR 1900+14 (De Luca et al. 2009), as well as the work by Motch et al. (2007), Motch et al. (2008), Kaplan et al. (2009), Becker et al. (2012), van Etten et al. (2012).

2.1. Chandra observations and data reduction

Our new observation of PSR J0357+3205 with *Chandra* was performed on 2011, December 24 (Obs.Id. 14007, 29.4 ks exposure time – hereafter tagged as “2011”). Previous observations were performed on 2009 October 25 (obs. id. 12008, 29.5 ks – hereafter “2009a”) and on 2009 October 26 (obs. id. 11239, 47.1 ks – hereafter “2009b”). All data were collected using the Advanced CCD Imaging Spectrometer (ACIS) instrument in Timed Exposure mode with the VFAINT telemetry mode. We retrieved “Level 1” data from the *Chandra* Science Archive and reprocessed them with the `chandra_repro`² script of the *Chandra* Interactive Analysis of Observation Software (CIAO v4.4)³.

For each observation, we generated an image in the 0.3–8 keV energy range using the original ACIS pixel size (0".492/pixel). We performed a source detection using the `wavdetect`⁴ task with wavelet scales ranging from 1 to 16 pixels with a $\sqrt{2}$ step size, setting a detection threshold of 10^{-6} . In all observations, the target was imaged close to the aimpoint, on the backside-illuminated chip S3 of the ACIS-S array.

We cross-correlated the resulting source lists using a correlation radius of 3" and we extracted a catalogue of common sources for each pair of observations. In view of the density of sources in each image, the possibility of a chance alignment of two false detections is $< 10^{-5}$. As a further step, we selected sources within 4' of the aimpoint since the telescope point spread function deteriorates as a function of offaxis angle, hampering source localization accuracy (see discussion in De Luca et al. 2009). Such an exercise yielded 12 common sources (2011 vs. 2009a), 10 sources (2011 vs. 2009b) and 16 sources (2009a vs.

²http://cxc.harvard.edu/ciao/ahelp/chandra_repro.html

³<http://cxc.harvard.edu/ciao/index.html>

⁴<http://cxc.harvard.edu/ciao/threads/wavdetect/>

2009b), in addition to the target pulsar. The uncertainty on the source localization on each image depends on the signal to noise as well as on the offaxis angle and ranges from ~ 0.08 to ~ 0.7 pixel per coordinate.

2.2. Relative astrometry

The positions of the selected, common sources (excluding the pulsar counterpart) were adopted as a reference grid to perform relative astrometry. We used the ACIS SKY reference system⁵ (pixel coordinates with axes aligned along Right Ascension and Declination). Taking into account the corresponding uncertainties, we computed the best geometric transformation needed to superimpose the reference frames of two images collected at different epochs.

We superimposed the most recent 2011 data to first-epoch 2009a and (separately) 2009b data in order to measure the possible pulsar displacement over a baseline of ~ 2.2 yr. We also superimposed 2009a data to 2009b data (no displacement is expected on a 1-day baseline) in order to check for systematics affecting our analysis. A simple translation yielded a good superposition in all cases (see Table 1). The uncertainty on the frame registration turned out to be smaller than 50 mas per coordinate. Adding a further free parameter to the transformation (a rotation angle) did not result in a statistically compelling improvement of the fit.

We applied the best-fit transformation to the coordinates of the pulsar counterpart and we computed its displacement between different epochs. The error budget for the overall pulsar displacement includes the uncertainty on the pulsar position in each image as well as the uncertainty on the multi-epoch frame registration. Results are shown in Table 1.

⁵<http://cxc.harvard.edu/ciao/ahelp/coords.html>

Table 1: Results of X-ray relative astrometry

	2011 vs. 2009a	2011 vs. 2009b	2009a vs. 2009b
Time baseline	2.16 yr	2.16 yr	1 day
Number of ref.srscs	11 ^a	10	16
uncertainty on X_{shift} (pixels)	0.09	0.08	0.06
χ^2 (dof)	13.6 (10)	15.6 (9)	7.8 (15)
uncertainty on Y_{shift} (pixels)	0.08	0.07	0.06
χ^2 (d.o.f.)	8.1 (10)	13.0 (9)	13.8 (15)
PSR X displacement (pixels)	0.53 ± 0.12	0.50 ± 0.11	0.10 ± 0.10
PSR Y displacement (pixels)	0.54 ± 0.11	0.50 ± 0.10	0.04 ± 0.10

^aA reference source yielding high residuals was rejected.

Displacement of the pulsar as well as residuals on the positions of the reference sources after frame registration are also shown in Figure 1. A significant and consistent displacement of the pulsar is apparent both in the 2011 vs. 2009a and in the 2011 vs. 2009b comparison, while no displacement is seen for the pulsar in the 2009a vs. 2009b one.

By combining the two measurements, we obtain a pulsar proper motion $\mu_\alpha \cos(\delta) = 117 \pm 20 \text{ mas yr}^{-1}$ and $\mu_\delta = 115 \pm 20 \text{ mas yr}^{-1}$. This corresponds to a total proper motion of $165 \pm 30 \text{ mas yr}^{-1}$, translating to a (projected) space velocity of $\sim 390 d_{500} \text{ km s}^{-1}$ (where d_{500} is the distance to the pulsar in units of 500 pc). The position angle of the proper motion is $314^\circ \pm 10^\circ$ (North to East) (see Figure 2). The proper motion direction is very well aligned with the main axis of the nebula, which is indeed an “X-ray trail”.

3. Gemini H_α observations.

We observed the field of PSR J0357+3205 in the H_α band on September 23, 2012 with the Gemini-North telescope on the Mauna Kea Observatory. We used the Gemini Multi-Object Spectrograph (GMOS) in its imaging mode equipped with the interim upgrade e2v deep depletion (DD) detector, with enhanced response in the blue and red arm of the spectrum with respect to the original EEV detector. The e2v DD detector is an array of three chips, with an unbinned pixel size of $0''.0728$ and covers an unvignetted field-of-view of $5'.5 \times 5'.5$. We used the Ha_G0310 filter ($\lambda = 656 \text{ nm}$; $\Delta\lambda = 7 \text{ nm}$), centered on the H_α rest wavelength. The e2v DD detector was set in the 2×2 binning mode and read through the standard slow read-out/low gain mode with the six amplifiers. Observations were performed with an average airmass of 1.24, image quality of $\sim 0''.8$, and grey time. Two sets of six 500 s exposures were obtained, for a total integration time of 6000 s. Exposures were dithered in steps of ± 5 pixels to achieve a better signal-to-noise (S/N).

We processed the GMOS images using the dedicated GMOS image reduction package available in IRAF. After downloading the closest bias and sky flat-field frames from the *Gemini* science archive⁶, we used the tasks `gbias` and `giflat` to process and combine the bias and flat-field frames, respectively. We then reduced the single science frames using the task `gireduce` for bias subtraction, overscan correction, image trimming and flat-field normalisation. From the reduced science images, we produced a mosaic of the three GMOS chips using the task `gmosaic` and we used the task `imcoadd` to average-stack the reduced image mosaics and filter out cosmic ray hits. We computed the astrometry calibration using the *wcstools*⁷ suite of programs, matching the sky coordinates of stars selected from the Two Micron All Sky Survey (2MASS) All-Sky Catalog of Point Sources (Skrutskie et al. 2006) with their pixel coordinates computed by *SExtractor* (Bertin & Arnouts 1996). After iterating the matching process applying a σ -clipping selection to filter out obvious mismatches, high-proper motion stars, and false detections, we obtained mean residuals of $\sim 0''.2$ in the radial direction, using up to 30 bright, but non-saturated, 2MASS stars. To this value we added in quadrature the uncertainty $\sigma_{tr} = 0''.08$ of the image registration on the 2MASS reference frame. This is given by $\sigma_{tr} = \sqrt{n/N_S} \sigma_S$ (e.g. Lattanzi et al. 1997), where N_S is the number of stars used to compute the astrometric solution, $n=5$ is the number of free parameters in the sky-to-image transformation model, $\sigma_S \sim 0''.2$ is the mean absolute position error of 2MASS (Skrutskie et al. 2006) for stars in the magnitude range $15.5 \leq K \leq 13$. After accounting for the $0''.015$ uncertainty on the link of 2MASS to the International Celestial Reference Frame (Skrutskie et al. 2006), we evaluated with the overall accuracy on our absolute astrometry to be of $\sim 0''.22$.

Unfortunately, no observations of spectro-photometric standards stars were available

⁶<http://cadwww.dao.nrc.ca/gsa/>

⁷<http://tdc-www.harvard.edu/wcstools/>

for the flux calibration of our H_α image. Thus, we cross-correlated instrumental magnitudes of more than 150 non-saturated stars in the Gemini image to their R_F magnitudes listed in the Guide Star Catalogue v2.3.2 (GSC2, Lasker et al. 2008), which yielded a rather good fit with a r.m.s. of 0.16 mag. To assess the GSC2 flux zeropoint, we cross-correlated the GSC2 R_F magnitude of more than 500 stars with their R magnitude as tabulated in the Stetson Standard photometric star archive⁸. We evaluated the transformation as $R_F=0.97R-0.32$ ($\chi^2 = 617, 520$ d.o.f.). Then, we computed the H_α fluxes of the 150 selected stars on our Gemini image using specific fluxes corresponding to their R_F magnitudes and assuming a flat spectrum within the R filter bandpass. This yielded a flux calibration of the H_α image with an uncertainty of ~ 0.2 mag.

No structures of diffuse emission unambiguously related to the fast motion of PSR J0357+3205 can be discerned on our Gemini image – in particular, no arc-shaped “bow-shock” nebula is seen at the expected position in the direction of the pulsar proper motion (see Figure 3). We measured the background properties in the region surrounding the pulsar position. Considering a region of 10 square arcsec as a reference and taking into account the uncertainty in the flux calibration of our H_α image, we computed the 5σ upper limit to the surface brightness of an unseen bow-shock nebula to be of 5×10^{-18} erg cm⁻² s⁻¹ arcsec⁻².

4. Discussion

Relative astrometry on our multi-epoch *Chandra* images unveiled a significant proper motion of 165 ± 30 mas yr⁻¹ for PSR J0357+3205, corresponding to a velocity of ~ 390 d₅₀₀ km s⁻¹, along a direction almost coincident with the main axis of the elongated X-ray

⁸<http://www3.cadc-ccda.hia-ihp.nrc-cnrc.gc.ca/community/STETSON/archive/>

nebula.

Our result points to a direct link between the nebula morphology (and physics) and the space velocity of the pulsar – supersonic for any reasonable condition of the interstellar medium (typical values are of ~ 1 , ~ 10 and $\sim 100 \text{ km s}^{-1}$ for the cold, warm and hot components, respectively, see e.g. Kulkarni & Heiles 1988). As already mentioned, “velocity-driven” pulsar wind nebulae are a well-known astrophysical reality. Could the X-ray trail of PSR J0357+3205 be explained as a bow-shock PWN? As discussed by De Luca et al. (2011), the lack of any evidence of the pulsar wind termination shock could be due to its confusion with the pulsar emission. Assuming a velocity of $390d_{500} \text{ km s}^{-1}$ and no inclination with respect to the plane of the sky, the expected angular separation between the pulsar and the forward and backward termination shock is $0''.3n_{1,ISM}^{-1/2}$ and $2''n_{1,ISM}^{-1/2}$, respectively (De Luca et al. 2011), where $n_{1,ISM}$ is the density of the interstellar medium in units of $1 \text{ particle cm}^{-3}$. Thus, high inclination of the pulsar velocity and/or high density of the ISM, and/or a distance larger than expected should be assumed; any of these hypotheses could be possible (though rather unlikely). In any case, other peculiarities of the trail phenomenology cannot be accounted for in the standard scenario of synchrotron emission from shocked pulsar wind. One should explain why the maximum luminosity is generated at a distance as large as ~ 3 light years from the parent neutron star. This would require an increase of the density of the radiating particles on the same distance scale (possibly due to deceleration of the bulk flow?), or an increase of the magnetic field intensity, or a change of the angle between the magnetic field and the particle flow. Moreover, the lack of any spectral steepening across the trail (De Luca et al. 2011) clashes with the expected, severe synchrotron energy losses of particles radiating in the keV range. Thus, either some very peculiar phenomenon is occurring in the magnetized pulsar particle outflow (local particle re-acceleration? large-scale organization of the flow magnetic field?) or the nature of the nebula is different (but linked to the pulsar velocity). For instance, Marelli et al. (2012)

propose that the trail could be due to thermal emission by the ISM heated by the shock driven by the fast moving pulsar.

The measure of the pulsar space velocity can be used, together with the upper limit to the surface brightness of any undetected diffuse structure in our Gemini H_α image, to constrain the conditions of the medium in which PSR J0357+3205 is moving. The expected flux of the narrow-line component of a pulsar H_α bow-shock nebula depends on the pulsar spin-down luminosity \dot{E}_{rot} , the pulsar space velocity v_{psr} , the distance to the source D_{psr} , and the neutral fraction of the medium X_{ISM} . Using the scaling law proposed by Cordes et al. (1993) and Chatterjee & Cordes (2002), we estimated that for any reasonable value of the distance to PSR J0357+3205 (ranging from ~ 200 pc, as suggested by the non negligible X-ray absorbing column, to ~ 900 pc, where γ -ray luminosity would exceed the spin-down luminosity) and in a broad range of possible space velocities for the pulsar (assuming the inclination angle with respect to the plane of the sky in the $\pm 75^\circ$ range), the lack of detection of a H_α nebula can only be ascribed to a neutral fraction $X_{ISM} < 0.01$, i.e. the gas surrounding the pulsar is fully ionized. Thus, PSR J0357+3205 could be traveling across a region filled with ISM in the hot phase. Some contribution to the ionization of the medium from the pulsar itself is also possible, although its thermal emission is not particularly prominent (De Luca et al. 2011).

PSR J0357+3205 is located well away from the Galactic plane ($b \sim -16^\circ$). In view of this, it is interesting to note that the direction of the pulsar proper motion is almost parallel to the Galactic plane (it has an inclination of $\sim 2^\circ$ towards the Plane). As done in Mignani et al. (2012), we used the proper motion information to extrapolate back in time the trajectory of the pulsar in the Galactic potential to find possible associations with open clusters and OB associations (Dias et al. 2002; Melnik et al. 2009; de Zeeuw et al. 1999), leaving the pulsar radial velocity as a free parameter and assuming a distance of 500 pc

and an age of 0.54 Myr. However, we found no association with clusters or OB associations closer than ~ 2 kpc. In any case, such an exercise showed us that if PSR J0357+3205 has a radial velocity of order 600 km s^{-1} (or greater) in the direction away from the Solar System, the pulsar could have been born on the Galactic plane (assuming a scale height of 60 pc, typical for massive stars, see e.g. Maiz-Apellaniz 2001). Thus, the hypothesis of a runaway high-mass star as the progenitor of PSR J0357+3205, suggested by De Luca et al. (2011), is not required in a range of possible orbital solutions.

5. Conclusions

The radio-quiet PSR J0357+3205 is traveling very fast ($\sim 390 \text{ km s}^{-1}$) into a fully ionized interstellar medium. Its proper motion is perfectly aligned with its very elongated X-ray nebula, pointing to a physical link between the nebula and the space velocity of the neutron star. However, the standard scenario of a bow-shock synchrotron-emitting nebula does not explain the phenomenology of our target. Deep radio polarization images could help explain the nature of this PWN, by tracing the underlying large-scale magnetic field configuration. Unveiling a population of energetic, nearby pulsars missed by radio surveys, the *Fermi* mission is opening new avenues to detect unusual PWNe which could point to different ways to deposit pulsar rotational energy into the interstellar medium.

RPM thanks Andrew Gosling for his support during the preparation of the Gemini observations. The research leading to these results has received funding from the European Commission Seventh Framework Programme (FP7/2007-2013) under grant agreement n. 267251. This research used the facilities of the Canadian Astronomy Data Centre operated by the National Research Council of Canada with the support of the Canadian Space Agency.

Facilities: CXO (ACIS) Gemini:Gillett.

REFERENCES

- Abdo, A.A., et al., 2009a, *Science*, 325, 840
- Abdo, A.A., et al., 2009b, *ApJS*, 183, 46
- Atwood, W.B., et al. 2009, *ApJ*, 697, 1071
- Bandiera, R., 2008, *A&A*, 490, L3
- Becker, W., Prinz, T., Winkler, P.F., Petre, R., 2012, *ApJ* 755, 141
- Bertin E. & Arnouts S., 1996, *A&A Suppl.*, 117, 393
- Chatterjee, S., & Cordes, J.M., 2002, *ApJ*, 575, 407
- Cordes, J.M., Romani, R.W., Lundgren, S.C., 1993, *Nature* 362, 133
- De Luca, A., Marelli, M., Mignani, R.P., et al., 2011, *ApJ*, 733, 104
- de Luca, A., Caraveo, P.A., Esposito, P., Hurley, K., 2009, *ApJ*, 692, 158
- de Zeeuw, P. T., Hoogerwerf, R., de Bruijne, J.H.J., et al., 1999, *AJ*, 117, 354
- Dias, W.S., Alessi, B.S., Moitinho, A., Lepine, J.R.D., 2002, *A&A*, 389, 871
- Gaensler, B.M. & Slane, P.O., 2006, *ARA&A*, 44, 17
- Hui, C.Y., Huang, R.H.H., Trepl, L., et al., 2012, *ApJ* 747, 74
- Hui, C.Y. & Becker, W., 2007, *A&A*, 467, 1209
- Kaplan, D.L., Chatterjee, S., Hales, C.A., Gaensler, B.M., Slane, P.O., 2009, *AJ*, 137, 354
- Johnson, S.P. & Wang, Q.D., 2010, *MNRAS* 408, 1216

- Kargaltsev, O., & Pavlov, G. G. 2008a, in AIP Conf. Proc. 983, 40 Years of Pulsars: Millisecond Pulsars, Magnetars and More (Melville, NY: AIP), 171
- Kulkarni, S.R.& Heiles, C., 1988, in “Galactic and extragalactic radio astronomy (2nd edition)” (A89-40409 17-90). Berlin and New York, Springer-Verlag, 1988, p.95
- Lasker, B.M., Lattanzi, M.G., McLean, B.J., 2008, AJ, 136, 735
- Lattanzi M. G., Capetti A., & Macchetto F. D. 1997, A&A, 318, 997
- Maíz-Apellániz, J., 2001, AJ, 121, 2737
- Marelli, M., De Luca, A., Salvetti, D., et al., 2012, submitted to ApJ
- Mason, B.D., Henry, T.J, Hartkopf, W.I., William, I., ten Brummelaar, T., Soderblom, D.R., 1998, AJ, 116, 2975
- Melník, A. M. & Dambis, A.K., 2009, MNRAS, 400, 518
- Mignani, R. P., Vande Putte, D., Cropper, M., et al., 2012, MNRAS, in press, arXiv:1212.3141
- Motch, C., Pires, A.M., Haberl, F., Schwöpe, A., 2007, Ap&SS, 308, 217
- Motch, C., Pires, A.M., Haberl, F., Schwöpe, A., Zavlin, V.E., 2008, AIPC, 983, 354
- Ray, P.S., Kerr, M., Parent, D., Abdo, A.A., Guillemot, L., et al., 2011, ApJS 194, 17
- Skrutskie M. F., Cutri R. M., Stiening R., et al. 200 6, AJ, 131, 1163
- Van Etten, A., Romani, R.W., Ng, C.-Y., 2012, ApJ, 755, 151

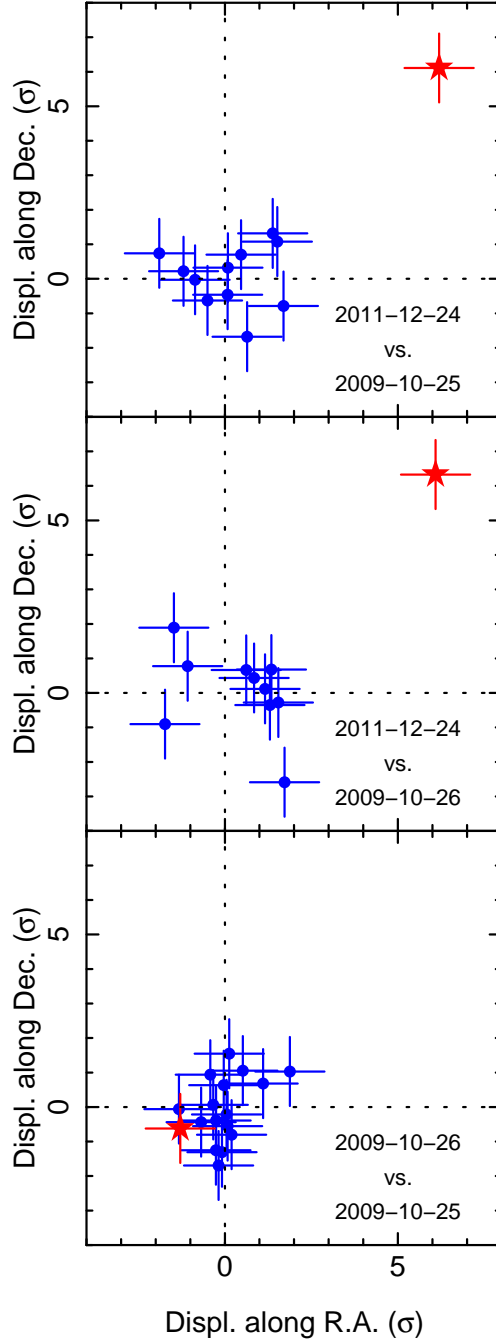


Fig. 1.— Results of relative astrometry. Two independent, first-epoch images (2009 October 25 and 2009 October 26) are compared to a second-epoch image (2011 December 24) in the upper and middle panels, respectively. Coordinate residuals after image superposition are shown for reference sources (blue dots) as well as for the pulsar counterpart (red star), in units of statistical errors. The displacement of the pulsar is apparent. The bottom box displays the comparison of the two first-epoch images showing, as expected, no displacements for any source.

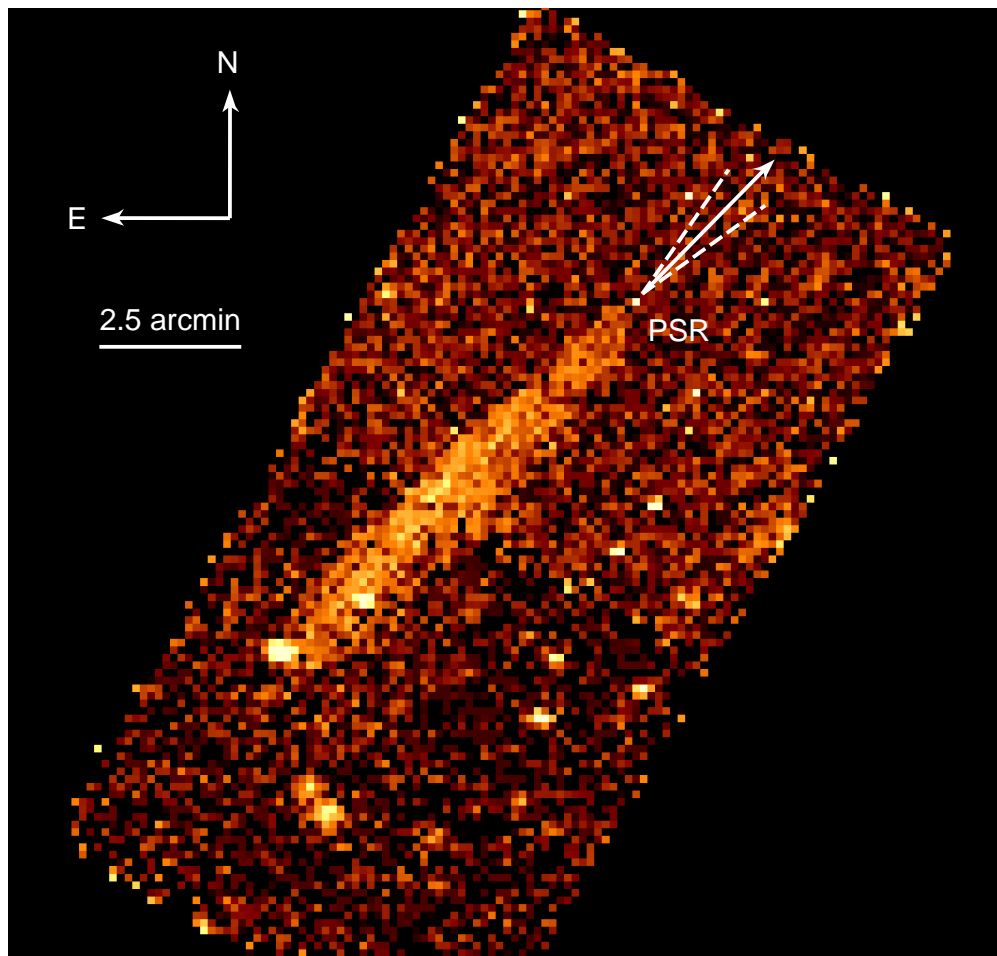


Fig. 2.— The field of PSR J0357+3205 as seen by Chandra in the 0.3-8 keV energy range. Data from the two observations performed in 2009 have been used (77 ks exposure time). The image has been rebinned to a pixel size of $8''$ in order to ease visibility of faint diffuse structures. The large, elongated nebula is apparent. The pulsar counterpart is marked, together with the direction of the proper motion (arrow) and the 1σ errors (dashed lines).

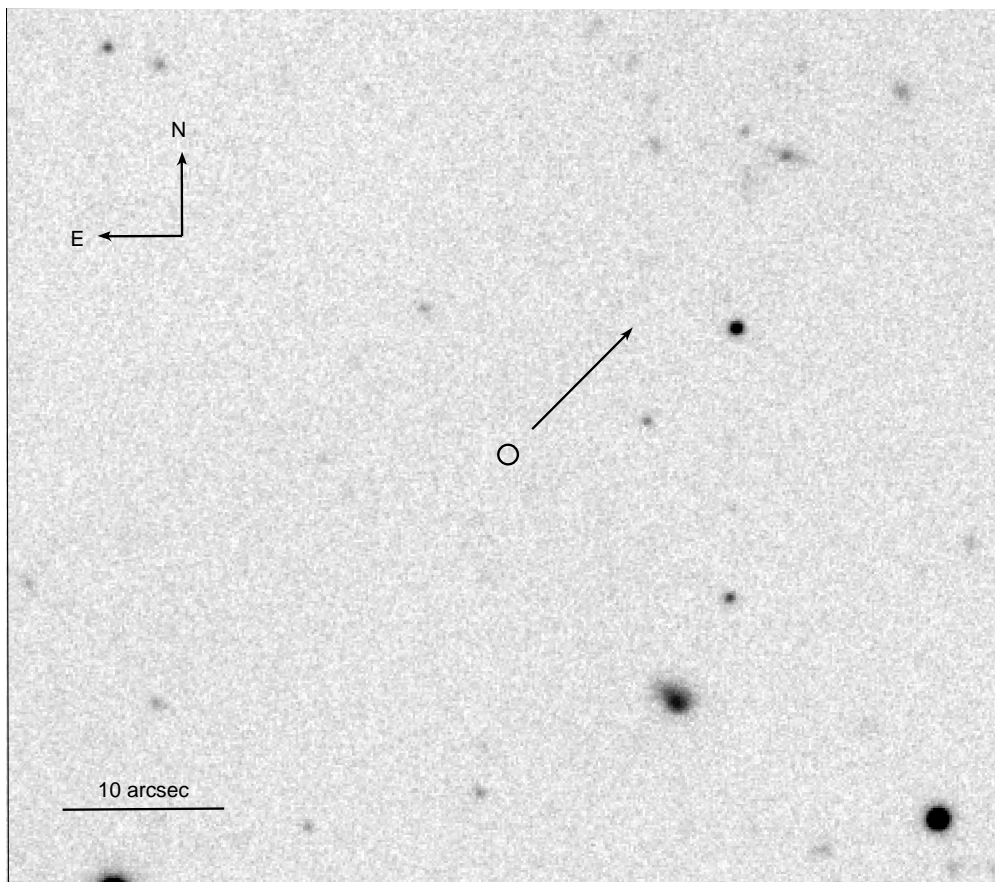


Fig. 3.— Inner portion of the field of PSR J0357+3205 as seen by the Gemini/GMOS instrument in the H_α band. The position of the pulsar is marked by a circle ($0''.6$ radius). No diffuse emission is seen, related to the proper motion direction of the pulsar, marked by an arrow. The upper limit to an undetected bow-shock nebula is $5 \times 10^{-18} \text{ erg cm}^{-2} \text{ s}^{-1} \text{ arcsec}^{-2}$.